Aerotecnica Missili & Spazio (2020) 99:287–295
https://doi.org/10.1007/s42496-020-00067-x

ORIGINAL ARTICLE

A 2-D Trajectory Design Algorithm for Multiple Asteroid Flyby Missions

Giuseppe Cataldi[1] · **Salvo Marcuccio**[1]

Received: 24 September 2020 / Revised: 21 October 2020 / Accepted: 26 October 2020 / Published online: 12 November 2020

Abstract
Asteroid mining is one of the most promising private space ventures of the near future. Near-Earth Asteroids (NEAs), i.e. those with perihelion at less than 1.3 AU from the Sun, are among the best candidates for such venture. In preparation of mining expeditions, it is likely that prospector missions will be carried out well in advance so to assess the accessibility, potential for revenues and possible critical issues of target asteroids. This work is concerned with the problem of the feasibility of a single spacecraft prospector mission capable of visiting as many NEAs as possible in one shot, focusing on Apollo-class asteroids only. The search of possible trajectories is done assuming a chemically propelled spacecraft with realistic specific impulse and propellant mass ratio, so to allow for a credible mission design with a reasonable, cost-effective total duration. In order to restrict the number of possible trajectories, only those that lie in the plane of the ecliptic are examined; such trajectories can be reached from the Earth without expensive plane change maneuvers. The search for a maximum number of encounters is thus restricted to those occurring where the asteroid orbit crosses the ecliptic. A deterministic building blocks approach is adopted, dividing the optimization problem in two parts: a local optimization for possible target determination; and a global optimization for the choice of the overall trajectory. It is found that the combined approach leads to the identification of viable trajectories, able to perform a number of encounters that depends on the launch epoch; as an example, in one test case two different sets of 21 NEA's each were identified that could be reached with a single launch, with a slightly different propellant expenditure. It is concluded that the method is well suited to perform feasibility studies of NEA missions with good accuracy and moderate computational cost.

Keywords Asteroid mining · Asteroid prospector · Asteroid flyby

1 Introduction

Near-Earth Asteroids (NEAs) are defined as those asteroids with a perihelion distance of less than 1.3 AU (astronomical unit). In recent years the interest in such objects has considerably increased, both for scientific and industrial purposes [1]: a better knowledge of the smaller bodies is essential to extend our understanding of the birth and evolution of the solar system; and the possibility to open up a wholly new market based on the exploitation of asteroid mineral resources is bringing around the birth of a new area of private space industry. Among NEAs, those with orbits crossing the Earth's orbit and a semi-major axis larger than the Earth's one are identified as members of the *Apollo* group. Such asteroids are quite interesting targets for mining ventures, as their relative proximity to the Earth makes them, in principle, easier to access than the other NEAs. In order to prepare properly for successful commercial exploitation of the awaiting riches, it is very likely that future space miners will want to carry out a number of exploratory missions, so to gather important information on the composition, size, shape, spin rate, etc. of the target bodies.

The study is aimed at assessing the requirements, the constraints and the feasibility, in terms of trajectory, of a prospecting mission capable to visit the largest possible number of Apollo asteroids with a single spacecraft. A visit is defined as a flyby at a distance sufficiently close so to allow for observation. The task is not trivial, due to the great number of the Apollo asteroids (Fig. 1), so to require the formulation of a dedicated method for the resolution of the

✉ Giuseppe Cataldi
giuseppe.cataldi@dici.unipi.it

Salvo Marcuccio
salvo.marcuccio@unipi.it

[1] Aerospace Division, Department of Civil and Industrial Engineering, University of Pisa, Via G. Caruso 8, 56122 Pisa, Italy

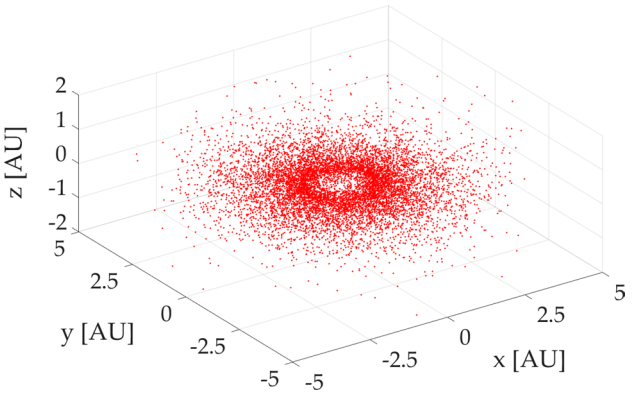

Fig. 1 Apollo asteroids at a generic time in the heliocentric-ecliptic reference frame

optimization problem about the selection of targets. In our study, it is explicitly assumed that our prospector spacecraft is propelled by chemical rockets, contrary to several recent works in the literature, where a similar *asteroid tour* problem is studied for low-thrust propelled spacecraft, either electrical [2, 3], or solar-sailing [4]. Moreover, this type of optimization problem is often solved by heuristic *genetic algorithms* [5] that allow to evaluate a set of initial solutions, and, introducing "disorder" elements, are able to create new solutions following an evolutionary path. The computational cost for very complex problems is therefore reduced; however, the method does not guarantee that an acceptable solution will be found. In this paper, a deterministic *building blocks* approach [3] is adopted, dividing the optimization problem in two parts: a local optimization to determine the next target; a global optimization to select the best visiting sequence. Data of the Apollo asteroids (and Earth) are retrieved from [6] and [7], respectively, and are relative to an heliocentric-ecliptic reference frame in the epoch J2000. The asteroid database is daily-updated with data about new bodies discovered, so that the proposed algorithm might produce very different results at different times in the future. A first version of the algorithm has been implemented in MATLAB® to analyze some test cases.

2 Assumptions

The starting data are the set of Keplerian orbital elements $\{a, e, i, \Omega, \omega\}$ (respectively semi-major axis, eccentricity, inclination, longitude of the ascending node and argument of periapsis) and the epoch of osculation t_{ref} with the relative asteroid position expressed by the mean anomaly M_{ref}, retrieved from [6]. Firstly, it is assumed that the asteroids trajectories are not affected by perturbations from other bodies (Keplerian orbits), so that *the asteroid orbital elements stay constant during the mission*. It can be seen from the

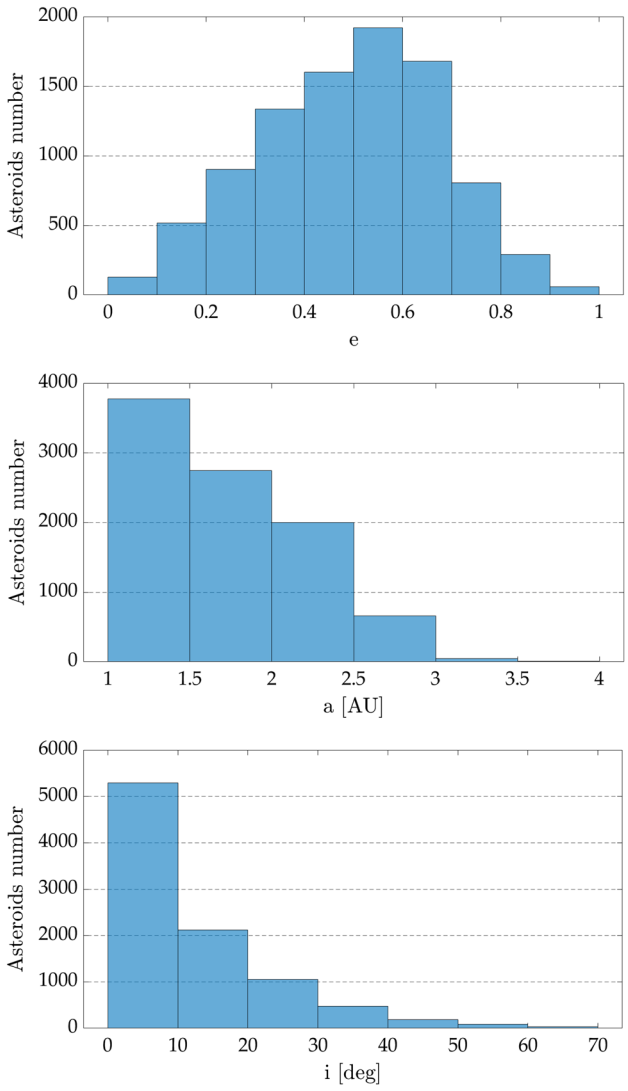

Fig. 2 Distribution of orbital parameters among Apollo asteroids, after data from [6]

distribution of these values among the asteroids (Fig. 2) that most of the asteroids have slightly inclined orbits; therefore it was chosen a trajectory lying on the ecliptic plane for the visiting spacecraft, in order to simplify the problem and to minimize inclination changes together with required propellant. With these assumptions, the problem is reduced to finding a step-by-step defined trajectory that starts from the Earth (after the escape) and intercepts the asteroids at their transit points on the ecliptic plane. Each overall trajectory's segment, joining two asteroids and followed by the spacecraft, will be a Keplerian arc with the necessary properties. Moreover, in the heliocentric phase, *all the maneuvers are assumed impulsive* without considering mass changes of the spacecraft and neglecting the details of what happens during the flyby phase. The main idea is to use a *building blocks* approach [3], in which the design of a complex trajectory

is the result of an assembly of optimal solutions to smaller problems, as will be explained later in detail.

3 Preliminary Phase

The first building block concerns the use of asteroids reference data (time, t_{ref}, and position, M_{ref}) in order to determine the transit positions on the ecliptic plane. It can be easily seen that the condition of transit is expressed in terms of the related true anomaly ν_{tr} by considering the reference frame transformation from perifocal to the heliocentric–ecliptic:

$$\begin{cases} x = r(\nu)[(\cos\Omega\cos\omega - \sin\Omega\sin\omega\cos i)\cos\nu + (-\cos\Omega\sin\omega - \sin\Omega\cos\omega\cos i)\sin\nu] \\ y = r(\nu)[(\sin\Omega\cos\omega + \cos\Omega\sin\omega\cos i)\cos\nu + (-\sin\Omega\sin\omega + \cos\Omega\cos\omega\cos i)\sin\nu] \\ z = r(\nu)[\sin\omega\sin i\cos\nu + \cos\omega\sin i\sin\nu] \end{cases};$$

with

$$r(\nu) = \frac{a\left(1-e^2\right)}{1+e\cos\nu};$$

and imposing:

$$z = 0 \;\Rightarrow\; \sin\omega\cos\nu_{tr} + \cos\omega\sin\nu_{tr} = 0 \;\Rightarrow\; \tan\nu_{tr} = -\tan\omega$$
$$\Rightarrow \left\{\nu_{tr}^{(1)}, \nu_{tr}^{(2)}\right\} \in [0, 2\pi),$$

with $\nu_{tr}^{(1)} < \nu_{tr}^{(2)}$. Two values of true anomaly result from this equation, each of them related to the position and velocity vectors, $\left\{\mathbf{r}_{tr}^{(1)}, \mathbf{r}_{tr}^{(2)}\right\}$ and $\left\{\mathbf{v}_{tr}^{(1)}, \mathbf{v}_{tr}^{(2)}\right\}$, found by solving an initial value problem, the *Direct Kepler's Problem* (DKP). It can be seen that the most of asteroids pass through the ecliptic plane at a distance from the Sun of about 1 AU, in a region named ***high-density transit zone*** (HDTZ) (Fig. 3)

Four quantities are available to the user to choose as input parameters:

- *Mission lifetime* $\left[t_0, t_{end}\right]$: expressed by mission start and end times;
- *Mission area* $\left[d_{min}, d_{max}\right]$: expressed by spacecraft-Sun minimum and maximum distances;
- *Maximum consumption per maneuver* Δv_{max}: index of propellant management for a single spacecraft maneuver;
- *Maximum mission consumption* Δv_{tot}: index of the on-board propellant at the start of the mission.

In this part of the analysis only the first two parameters are used, while the others will be useful later. Mission lifetime is critical for knowing the order and the date of transits. In particular, this phase concerns only the first and the second transits according to a temporal order. For this purpose, the initial position of asteroids is found in terms of true anomaly $\nu_0 = \nu\left(t_0\right)$ by solving another initial value problem, the *Reverse Kepler's Problem* (RKP). Hence, a new DKP is resolved with respect to the initial time t_0 to determine the dates of transit. Assuming as notation that the apex roman number expresses temporal order, three cases must be considered (n is the asteroid mean motion):

- Case 1

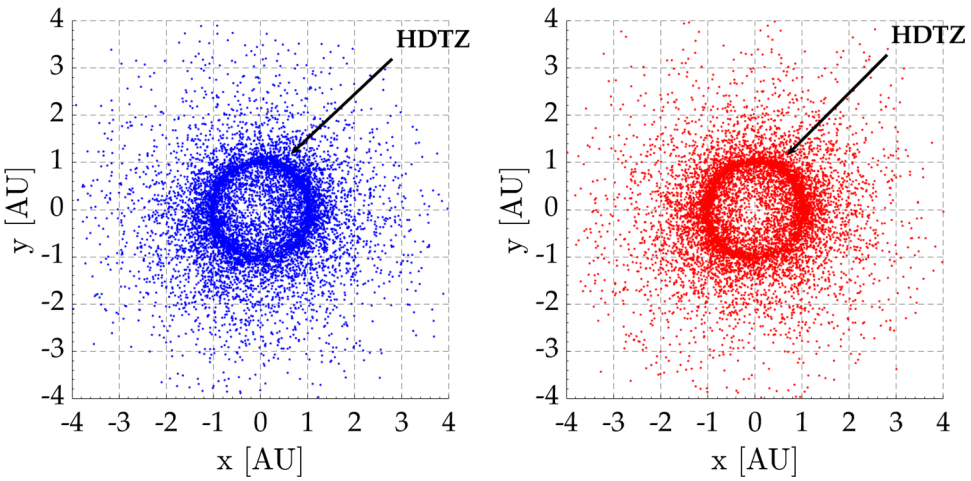

Fig. 3 Asteroid transition positions $\mathbf{r}_{tr}^{(1)}$ (left) and $\mathbf{r}_{tr}^{(2)}$ (right) on the ecliptic plane in the heliocentric-ecliptic reference frame

$$\text{if } 0 < \nu_0 < \nu_{\text{tr}}^{(1)} \Rightarrow \begin{cases} \mathbf{r}_{\text{tr}}^{I} = \mathbf{r}_{\text{tr}}^{(1)} \\ \mathbf{r}_{\text{tr}}^{II} = \mathbf{r}_{\text{tr}}^{(2)} \end{cases}$$

$$\Rightarrow \begin{cases} t_{\text{tr}}^{I} = t_0 + \left(M_{\text{tr}}^{(1)} - M_0\right)/n \\ t_{\text{tr}}^{II} = t_0 + \left(M_{\text{tr}}^{(2)} - M_0\right)/n \end{cases};$$

– Case 2

$$\text{if } \nu_{\text{tr}}^{(1)} < \nu_0 < \nu_{\text{tr}}^{(2)} \Rightarrow \begin{cases} \mathbf{r}_{\text{tr}}^{I} = \mathbf{r}_{\text{tr}}^{(2)} \\ \mathbf{r}_{\text{tr}}^{II} = \mathbf{r}_{\text{tr}}^{(1)} \end{cases}$$

$$\Rightarrow \begin{cases} t_{\text{tr}}^{I} = t_0 + \left(M_{\text{tr}}^{(2)} - M_0\right)/n \\ t_{\text{tr}}^{II} = t_0 + \left(M_{tr}^{(1)} + 2\pi - M_0\right)/n \end{cases};$$

– Case 3

$$\text{if } \nu_{\text{tr}}^{(2)} < \nu_0 < 2\pi \Rightarrow \begin{cases} \mathbf{r}_{\text{tr}}^{I} = \mathbf{r}_{\text{tr}}^{(1)} \\ \mathbf{r}_{\text{tr}}^{II} = \mathbf{r}_{\text{tr}}^{(2)} \end{cases}$$

$$\Rightarrow \begin{cases} t_{\text{tr}}^{I} = t_0 + \left(M_{\text{tr}}^{(1)} + 2\pi - M_0\right)/n \\ t_{\text{tr}}^{II} = t_0 + \left(M_{\text{tr}}^{(2)} + 2\pi - M_0\right)/n \end{cases}.$$

Finally, with the purpose of reducing the computational cost, the asteroids that transit too far in time and in space will not be considered from now on. Therefore, the ***potentially observable asteroids*** are defined as *the asteroids that transit at least once in the chosen area during the mission*. They must satisfy the following conditions:

$$\begin{cases} t_0 < t_{\text{tr}}^{I} < t_{\text{end}} \quad \text{or} \quad t_0 < t_{\text{tr}}^{II} < t_{\text{end}} \\ d_{\min} < |\mathbf{r}_{\text{tr}}^{I}| < d_{\max} \quad \text{or} \quad d_{\min} < |\mathbf{r}_{\text{tr}}^{II}| < d_{\max} \end{cases}. \tag{1}$$

The previous relations give the initial set of N asteroids that will be the subject of the algorithm in the next phases.

By indicating with N_{tot} the total number of asteroids discovered and reported in [6], the preliminary phase can be summarized as follows.

$\{a_k, e_k, i_k, \Omega_k, \omega_k\}$ and $t_{\text{ref},k}, M_{\text{ref},k}$ for $k = 1 : N_{\text{tot}}$ from [6];
$\{a_\oplus, e_\oplus, i_\oplus, \Omega_\oplus, \omega_\oplus\}$ and $t_{\text{ref},\oplus}, M_{\text{ref},\oplus}$ from [7];
$\tan \nu_{\text{tr},k} = -\tan \omega_k \Rightarrow \left(\nu_{\text{tr},k}^{(1)}, \nu_{\text{tr},k}^{(2)}\right)$ for $k = 1 : N_{\text{tot}}$;
$DKP \Rightarrow \left(\mathbf{r}_{\text{tr},k}^{(1)}, \mathbf{r}_{\text{tr},k}^{(2)}, \mathbf{v}_{\text{tr},k}^{(1)}, \mathbf{v}_{\text{tr},k}^{(2)}\right)$ for $k = 1 : N_{\text{tot}}$;
$RKP \Rightarrow (\mathbf{r}_{0,k}, \mathbf{v}_{0,k})$ for $k = 1 : N_{\text{tot}}$;
$RKP \Rightarrow (\mathbf{r}_{0,\oplus}, \mathbf{v}_{0,\oplus})$;
$DKP \Rightarrow \left(t_{\text{tr},k}^{I}, t_{\text{tr},k}^{II}, \mathbf{r}_{\text{tr},k}^{I}, \mathbf{r}_{\text{tr},k}^{II}, \mathbf{v}_{\text{tr},k}^{I}, \mathbf{v}_{\text{tr},k}^{II}\right)$ for $k = 1 : N_{\text{tot}}$;
$(1) \Rightarrow N$ asteroids.

4 Research Phase

This is the central core of the algorithm. Here, depending on the spacecraft position, the possible targets are determined. The starting variables are related to the current state of spacecraft: $(t, \mathbf{r}, \mathbf{v})$. At each generic iteration, a new calculation of the next transit data is needed for all the asteroids. Hence, a general method that comprises various cases and sub-cases is adopted as follows:

$$\text{if } t < t_{\text{tr}}^{I} \Rightarrow \begin{cases} t_{\text{tr}}^{\text{next}} = t_{\text{tr}}^{I} \\ \mathbf{r}_{\text{tr}}^{\text{next}} = \mathbf{r}_{\text{tr}}^{I} \\ \mathbf{v}_{\text{tr}}^{\text{next}} = \mathbf{v}_{\text{tr}}^{I} \end{cases};$$

a.

$$\text{if } t > t_{\text{tr}}^{I} \Rightarrow \lambda = (t - t_{\text{tr}}^{I}) \text{ div } T$$

$$\Rightarrow \begin{cases} \text{if } t < t_{\text{tr}}^{II} + \lambda T \Rightarrow \begin{cases} t_{\text{tr}}^{\text{next}} = t_{\text{tr}}^{I+2\lambda+1} = t_{\text{tr}}^{II} + \lambda T \\ \mathbf{r}_{\text{tr}}^{\text{next}} = \mathbf{r}_{\text{tr}}^{I+2\lambda+1} = \mathbf{r}_{\text{tr}}^{II} \\ \mathbf{v}_{\text{tr}}^{\text{next}} = \mathbf{v}_{\text{tr}}^{I+2\lambda+1} = \mathbf{v}_{\text{tr}}^{II} \end{cases} \\ \text{if } t > t_{\text{tr}}^{II} + \lambda T \Rightarrow \begin{cases} t_{\text{tr}}^{\text{next}} = t_{\text{tr}}^{I+2(\lambda+1)} = t_{\text{tr}}^{I} + (\lambda+1)T \\ \mathbf{r}_{\text{tr}}^{\text{next}} = \mathbf{r}_{\text{tr}}^{I+2(\lambda+1)} = \mathbf{r}_{\text{tr}}^{I} \\ \mathbf{v}_{\text{tr}}^{\text{next}} = \mathbf{v}_{\text{tr}}^{I+2(\lambda+1)} = \mathbf{v}_{\text{tr}}^{I} \end{cases} \end{cases}$$

b. (2)

where div represents the integer division operator, T is the asteroid period and λ is the number of periods elapsed since the first transition.

At this point it is convenient to introduce an ***observation area*** where the best trajectories linking spacecraft and asteroid's transit positions are evaluated. A spacecraft-centered semi-circular area in direction of the spacecraft velocity vector has been chosen. The radius is assumed according to

$$\delta = c_1 \min\left\{|\mathbf{r}_{\text{tr}}^{\text{next}} - \mathbf{r}|\right\}, \tag{3}$$

where c_1 is an arbitrary scale factor. With the right choice of c_1 it is possible to obtain a value of δ that ensures to consider a good number of asteroids around the spacecraft (Fig. 4). In the current case a scale factor of one order of magnitude seems to be a reasonable assumption: $c_1 = 10$.

From now on, there is the need of criteria forming a *funnel structure* (similar to *local minimizers* in [8]) to select the best targets. Firstly, only the asteroids that will perform the next transit inside the mission and the observation areas at the same time are considered:

$$\begin{cases} |\mathbf{r}_{\text{tr}}^{\text{next}} - \mathbf{r}| < \delta \\ d_{\min} < |\mathbf{r}_{\text{tr}}^{\text{next}}| < d_{\max} \end{cases};$$

Then, with the purpose to have orbits that stay as close as possible to the HDTZ, it is appropriate to choose only elliptical transfer orbits:

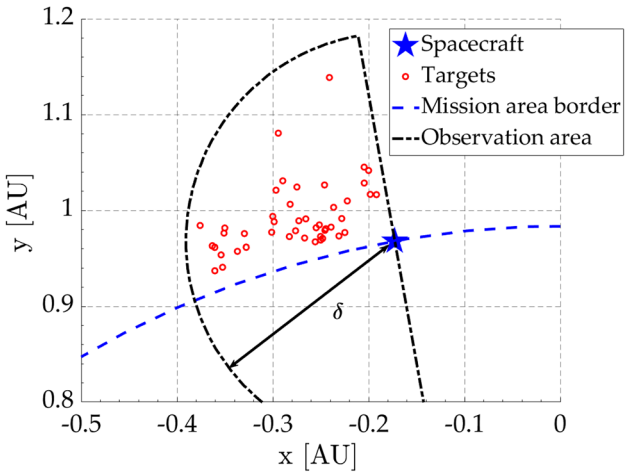

Fig. 4 Asteroids in the observation area during the initial step of the algorithm (spacecraft and Earth positions are the same). The mission area is defined as [1 AU, 1.5 AU], then the inner border corresponds to Earth's orbit

$$\Delta t = \left(t_{\text{tr}}^{\text{next}} - t\right) > t_p,$$

where Δt is the transfer time and t_p is the transfer time for the parabolic orbit. Simultaneously, it is required to minimize transfer time between two consecutive flybys by choosing the arc trajectory as short as possible. From Lambert's theory, there are four different elliptical trajectories that link two positions with a given transfer time. The selected trajectory arcs are those with

$$0 < \Delta\nu < \pi \quad \text{and} \quad \Delta t = \left(t_{\text{tr}}^{\text{next}} - t\right) < t_m,$$

where $\Delta\nu$ is the swept true anomaly and t_m is the transfer time for the minimum energy elliptical orbit. In this way only the shortest arcs are considered. Figure 5 shows the differences between the chosen and the rejected orbits: as it can be seen, the trajectories depicted in magenta would imply abrupt changes of direction at the next maneuver in order to maintain the spacecraft in the mission area.

At this point, for all the remaining asteroids a boundary value problem, the *Lambert's Problem* (LP), must be solved to get the transfer orbit parameters. Since the problem is ill-conditioned, it is better to make use of the universal variable formulation to achieve robustness. Hence, if two positions in space, $\mathbf{r}$ and $\mathbf{r}_{\text{tr}}^{\text{next}}$, linked by a trajectory with swept true anomaly $\Delta\nu$ and time Δt are considered, the solution z of LP is obtained by the equation:

$$\sqrt{\mu_\odot}\Delta t = \sqrt{\left(\frac{B}{C(z)}\right)^3} S(z) + A\sqrt{B};$$

with

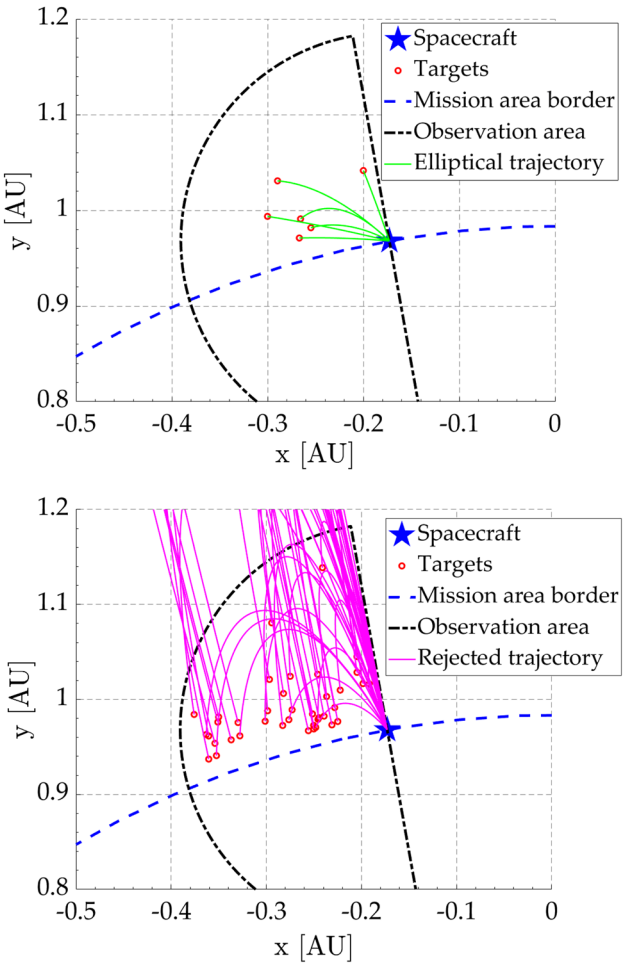

Fig. 5 Short elliptical arcs are depicted in green, while not favourable orbits are in magenta. The rejected trajectory arcs have greater specific orbital energy that requires a larger Δv for orbit insertion. Furthermore, the presence of a pronounced curvature would lead to an expensive maneuver to prevent the spacecraft from exiting the mission area

$$A = \frac{\sqrt{r\, r_{\text{tr}}^{\text{next}}}\sin\Delta\nu}{\sqrt{1-\cos\Delta\nu}}; \quad B = r + r_{\text{tr}}^{\text{next}} + A\frac{(zS(z)-1)}{\sqrt{C(z)}};$$
$$C(z) = \sum_{j=0}^{\infty}\frac{(-z)^j}{(2j+2)!}; \quad S(z) = \sum_{j=0}^{\infty}\frac{(-z)^j}{(2j+3)!}.$$

Then, the eccentricity and the semi-major axis of transfer orbit are obtained through

$$a_{\text{tr}} = \frac{y}{zC(z)}; \quad e_{\text{tr}} = \sqrt{1 - \frac{(1-\cos\Delta\nu)r\, r_{\text{tr}}^{\text{next}}}{y\, a_{\text{tr}}}}.$$

To compute the initial and final velocity vectors $\{\mathbf{v}_{\text{tr}}^{\text{in}}, \mathbf{v}_{\text{tr}}^{\text{fin}}\}$ along the arc, the expressions of the *Lagrangian coefficients* (LC) are used:

$$\mathcal{F} = 1 - \frac{r_{\text{tr}}^{\text{next}}(1-\cos \Delta\nu)}{a_{\text{tr}}\left(1-e_{\text{tr}}^2\right)}; \quad \mathcal{G} = \frac{r\, r_{\text{tr}}^{\text{next}} \sin \Delta\nu}{\sqrt{\mu_{\odot} a_{\text{tr}}\left(1-e_{\text{tr}}^2\right)}};$$

$$\dot{\mathcal{G}} = 1 - \frac{r(1-\cos \Delta\nu)}{a_{\text{tr}}\left(1-e_{\text{tr}}^2\right)}; \quad \dot{\mathcal{F}} = \frac{\mathcal{F}\dot{\mathcal{G}} - 1}{\mathcal{G}};$$

obtaining:

$$\mathbf{v}_{\text{tr}}^{\text{in}} = \frac{1}{\mathcal{G}}\left(\mathbf{r}_{\text{tr}}^{\text{next}} - \mathcal{F}\mathbf{r}\right) \quad \text{and} \quad \mathbf{v}_{\text{tr}}^{\text{fin}} = \dot{\mathcal{F}}\mathbf{r} + \dot{\mathcal{G}}\mathbf{v}_{\text{tr}}^{\text{in}}.$$

Finally, only the arc trajectories that are compatible with the spacecraft propellant consumption requirements are considered:

$$\Delta \text{v} = |\mathbf{v}_{\text{tr}}^{\text{in}} - \mathbf{v}| < \Delta \text{v}_{\max}.$$

In many cases, depending on the choice of user inputs, it may happen that no suitable target is found inside the observation area. In such cases, the algorithm will restart the selection using an increased observation area of radius:

$$\delta_{\text{new}} = c_2 \delta \quad \text{up to} \quad \delta_{\max} = 2d_{\max}; \tag{4}$$

where c_2 is an arbitrary magnification factor (in the current case $c_2 = 2$), while the imposed δ maximum value corresponds to the limit case in which the observation radius is as wide as the maximum mission distance from the Sun.

Summing up, the funnel structure of the preliminary phase is:

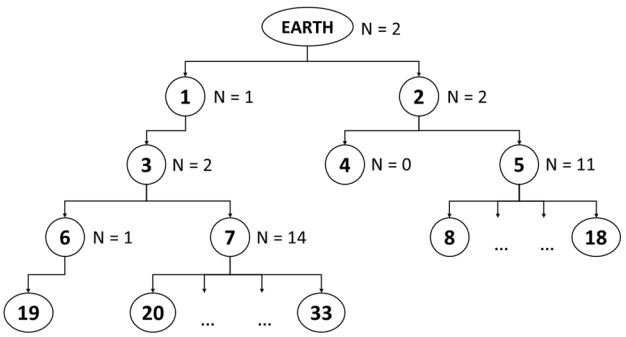

Fig. 6 Tree-structure diagram with $\mathbf{N}_{\text{bank}} = [2, 1, 2, 2, 0, 11, 1, 14]$. The order of exploration of nodes is indicated by the bold numbers in circles

At the end of the research phase, one of the final N_{fin} asteroids must be selected as target, following criteria discussed in the next section. Let $k = l$ be the index of the selected target, the next research phase iteration will have as input variables:

$$(t, \mathbf{r}, \mathbf{v}) = \left(t_{\text{tr},l}^{\text{next}}, \mathbf{r}_{\text{tr},l}^{\text{next}}, \mathbf{v}_{\text{tr},l}^{\text{next}}\right).$$

5 Implementation Strategy

Two possible paths are considered for the final selection of target. First, at every iteration the orbit with minimum Δv can be chosen. This strategy provides a low computational cost and a local optimization but not a global one for the mission, so it can be used when quick results are wanted. In the latter strategy the research iteration is used with the purpose to determine

Input variables: $(t, \mathbf{r}, \mathbf{v})$;
$(2) \Rightarrow \left(t_{\text{tr},k}^{\text{next}}, \mathbf{r}_{\text{tr},k}^{\text{next}}, \mathbf{v}_{\text{tr},k}^{\text{next}}\right)$ for $k = 1 : N$;
$(3) \Rightarrow \delta$;
$|\mathbf{r}_{\text{tr},k}^{\text{next}} - \mathbf{r}| < \delta$ for $k = 1 : N \Rightarrow N_1$ asteroids;
$d_{\min} < |\mathbf{r}_{\text{tr},k}^{\text{next}}| < d_{\max}$ for $k = 1 : N_1 \Rightarrow N_2$ asteroids;
$t_{\text{tr},k}^{\text{next}} - t > t_{p,k}$ for $k = 1 : N_2 \Rightarrow N_3$ asteroids;
$0 < \Delta\nu_k < \pi$ and $t_{\text{tr},k}^{\text{next}} - t < t_{m,k}$ for $k = 1 : N_3 \Rightarrow N_4$ asteroids;
$LP \Rightarrow (e_{\text{tr},k}, a_{\text{tr},k})$ for $k = 1 : N_4$;
$LC \Rightarrow \left(\mathbf{v}_{\text{tr},k}^{\text{in}}, \mathbf{v}_{\text{tr},k}^{\text{fin}}\right)$ for $k = 1 : N_4$;
$|\mathbf{v}_{\text{tr},k}^{\text{in}} - \mathbf{v}| < \Delta \text{v}_{\max}$ for $k = 1 : N_4 \Rightarrow N_{\text{fin}}$ asteroids;
if $N_{\text{fin}} = 0 \Rightarrow (4) \Rightarrow$ restart;
Output variables: $\left(t_{\text{tr},k}^{\text{next}}, \mathbf{r}_{\text{tr},k}^{\text{next}}, \mathbf{v}_{\text{tr},k}^{\text{next}}, e_{\text{tr},k}, a_{\text{tr},k}, \mathbf{v}_{\text{tr},k}^{\text{in}}, \mathbf{v}_{\text{tr},k}^{\text{fin}}\right)$ for $k = 1 : N_{\text{fin}}$.

all the possible trajectories combinations (*breadth first search* [3]), and then to find the best spacecraft orbit at the expense of a higher computational cost. In this way, a ***tree-structure*** result (Fig. 6) will be obtained; then, the combination of orbits that predicts the largest number of flybys and total minimum consumption, within the time limits of mission (*brunch and prune approach*), is selected [2]. In both cases, the procedure will stop working when it arrives at a time $t > t_{\text{end}}$ (time over) or when the total propellant consumption exceeds the expected one Δv_{tot} (propellant over).

In the present version of the algorithm, the tree search strategy is used. Because of its high computational cost, it is necessary to reduce the number of instructions when it is possible. For this reason, during the research phase it is preferable to work on temporary sets of data and, at the end, collect only the useful results in bank carriers arrays. Hence, the funnel selection is done by eliminating the components of a temporary vector $\mathbf{I}_{\text{temp}}$, whose generic component is the asteroid list index in [6]. The remaining components are collected in a related bank carrier and will act as identifiers of the target. In particular, the main bank carriers are:

- $\mathbf{N}_{\text{bank}}$: array whose i-th component is the number of possible targets found at the i-th iteration.
- $\mathbf{I}_{\text{bank}}$: array whose i-th component is the list index of the i-th asteroid found since the beginning of the procedure. As already mentioned, its components play the role of identifiers of target.
- $\mathbf{t}_{\text{bank}}$: array whose i-th component is the time of transit of the i-th target found since the beginning of the procedure.
- $\mathbf{r}_{\text{bank}}$: array whose i-th component is the position vector of the i-th target found since the beginning of the procedure.
- $\left\{\mathbf{v}^{\text{in}}_{\text{bank}}, \mathbf{v}^{\text{fin}}_{\text{bank}}\right\}$: arrays whose i-th component is respectively the initial and final velocity vector of the i-th maneuver found since the beginning of the procedure. These data are essential for the evaluation of consumption and the final selection of path.
- $\left\{\mathbf{e}_{\text{bank}}, \mathbf{a}_{\text{bank}}\right\}$: arrays whose i-th component is respectively the eccentricity and the semi-major axis of the i-th transfer orbit found since the beginning of the procedure.
- $\Delta\boldsymbol{\nu}_{\text{bank}}$: array whose i-th component is the swept true anomaly during the i-th transfer orbit found since the beginning of the procedure.

All the aforementioned bank carriers are essential for the reconstruction of trajectory. In particular, at the end of the procedure, the array $\mathbf{N}_{\text{bank}}$ is fundamental for the codification of the tree-structured results into a matrix J. Let's assume $\mathbf{N}_{\text{bank}} = \left[N_1, N_2, \ldots, N_H\right]$, it can be noted that

$$L = \sum_{k}^{H} N_k,$$

corresponds to the overall nodes number of the tree-structure, and, therefore, to the main size of the other bank carriers.

To explain the coding process, let's introduce a parameter M, that represents the *number of already converted nodes*. The procedure starts with a matrix

$$J_0 = \begin{pmatrix} 1 & 2 & \ldots & N_1 \end{pmatrix},$$

and a value of $M_0 = N_1$. From now on, the process continues iteratively. Let's assume a generic form of the matrix at the ith iteration:

$$J_i = \begin{pmatrix} J_{11} & J_{12} & \ldots & J_{1,\text{end}} \\ J_{21} & J_{22} & \ldots & J_{2,\text{end}} \\ \vdots & \vdots & \ddots & \vdots \\ J_{\text{end},1} & J_{\text{end},2} & \ldots & J_{\text{end,end}} \end{pmatrix},$$

with a given value of $M_i < L$.

Every column (i.e. from index 1 to end) is replaced, by the following submatrix:

a. if $N_{(J_{\text{end},j}+1)} \neq 0$ and $J_{\text{end},j} \neq 0$

$$\begin{pmatrix} J_{1j} & J_{1j} & \ldots & J_{1j} \\ \vdots & \vdots & \ddots & \vdots \\ J_{\text{end},j} & J_{\text{end},j} & \ldots & J_{\text{end},j} \\ M+S+1 & M+S+2 & \ldots & M+S+N_{(J_{\text{end},j}+1)} \end{pmatrix},$$

with

$$S = \sum_{k=0}^{j-1} N_{(J_{\text{end},k}+1)},$$

b. if $N_{(J_{\text{end},j}+1)} = 0$ or $J_{\text{end},j} = 0$

$$\begin{pmatrix} J_{1j} \\ \vdots \\ J_{\text{end},j} \\ 0 \end{pmatrix},$$

After a complete iteration there is a new row into the matrix and M is updated to a new value given by:

$$M_{i+1} = \max_{(i,j)} \left\{J_{i,j}\right\}.$$

For example, in relation to Fig. 6 the matrix appears as 4-by-27 in the following form:

$$J = \begin{pmatrix} 1 & 1 & \ldots & 1 & 2 & 2 & \ldots & 2 \\ 3 & 3 & \ldots & 3 & 4 & 5 & \ldots & 5 \\ 6 & 7 & \ldots & 7 & 0 & 8 & \ldots & 18 \\ 19 & 20 & \ldots & 33 & 0 & 0 & \ldots & 0 \end{pmatrix}.$$

The null terms in the matrix mean that the research phase did not produce any possible trajectory. Therefore, the columns

with zero terms are deleted in order to obtain the best trajectories in terms of number of asteroids. Finally, the column with the corresponding minimum Δv, representing the best overall trajectory, is selected.

6 Main Results

The algorithm was tested with the following input values:

- mission lifetime: $[t_0, t_{end}] = [t_0, t_0 + 5 \text{ years}]$;
- mission area: $[d_{min}, d_{max}] = [1, 1.5]$ AU;
- maximum consumption per maneuver: $\Delta v_{max} = 0.5$ km/s ;
- maximum mission consumption: $\Delta v_{tot} = 5.5$ km/s.

Several test cases have been tried with t_0 ranging from 1st of January 2020 to 1st of January 2030 with a six months step. The best results have been obtained with a launch window in January 2024 (see Table 1), showing that is possible to consecutively reach 21 asteroids with a consumption of 5.3 km/s. The final spacecraft trajectory is plotted in Fig. 7 (green). As expected, the trajectory lies in the HDTZ and has a smooth shape. Furthermore, for the same launch date, four other sequences consisting of 21 asteroids are obtained. One of these includes visits to asteroids with a completely different sequence (see Fig. 7; Table 1), with approximately the same Δv. As a result, it is possible to double the visits number by means of two prospector spacecrafts and with the same launch.

7 Conclusions

The algorithm has shown very good performance and a moderate computational cost, allowing for its use in the context of an asteroid mining pre-Phase A study carried out internally at the University of Pisa. In addition to identifying the mission profile, the provided results have been quite helpful for the preliminary design of various spacecraft subsystems. For example, the evaluation of the relative velocity between spacecraft and asteroid was used to establish the requirements for the ADCS (Attitude Determination and Control System) during the prospecting phase.

The algorithm is based on several assumptions and its results are at a medium level of accuracy. Further and more advanced versions of the code, e.g., including perturbation models, can be developed to increase the accuracy. Also, the procedure can be applied to similar problems after some adaptations, e.g., to the analysis of a different pool of celestial bodies or, in general, to space missions in Earth orbit involving multiple targets (such as mission dedicated to the removal of space debris [9]. Two noteworthy databases can be mentioned as examples of other target groups:

1. the *Near-Earth Object Human Space Flight Accessible Target Study (NHATS)*, introduced by [10], containing the possible NEA targets for a future manned mission; and

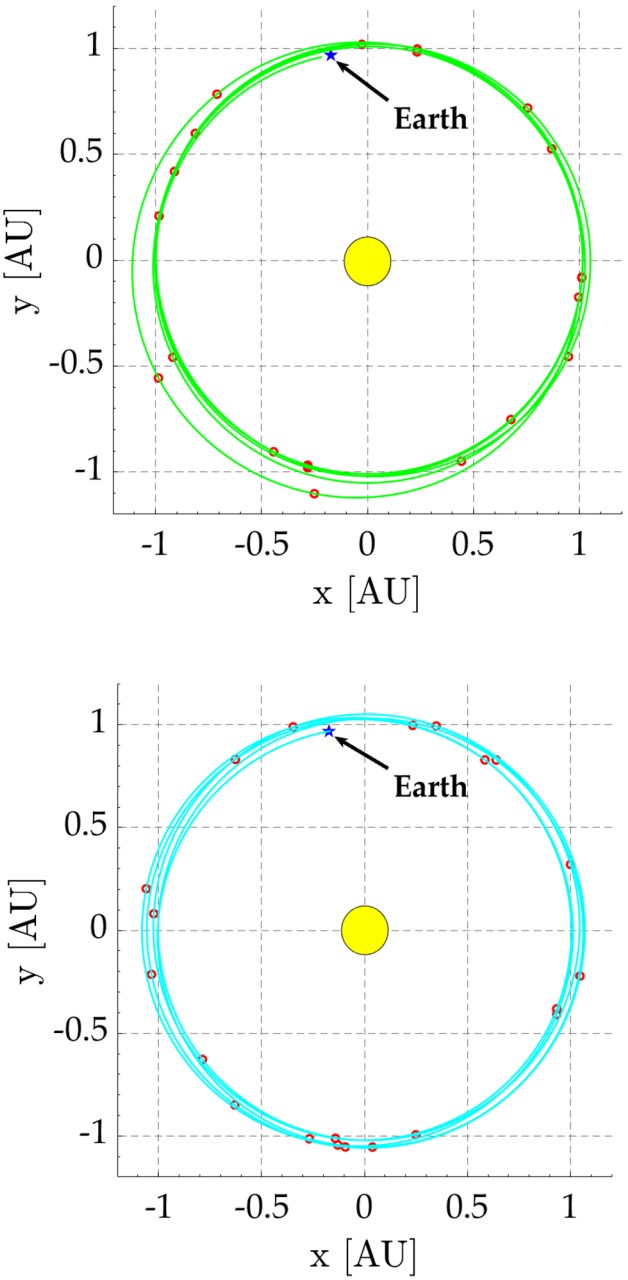

Fig. 7 Spacecraft trajectories. The first plot represents the best trajectory for a launch on 1th January 2024, the latter one is the other possible trajectory with different target asteroids. The blue cross represents the starting position (Earth) and the red circles the target asteroids

Table 1 Two possible set of targets. Both cases present 21 asteroids, with a total consumption $\Delta v_{tot} \approx 5.3$ km/s

First spacecraft		Second spacecraft	
Asteroid full name	Flyby date [DMY]	Asteroid full name	Flyby date [DMY]
(2016 LJ10)	8th June 2024	(2011 LZ2)	6th June 2024
(2017 MF3)	27th June 2024	(2015 SH)	20th September 2024
(2010 VB99)	30th November 2024	(2015 XX169)	12th December 2024
164207 (2004 GU9)	21st May 2025	(2014 DE23)	2nd March 2025
(2016 NO56)	28th July 2025	(2016 LR51)	10th June 2025
(2017 FP101)	5th November 2025	(2017 BW30)	9th August 2025
(2006 AS3)	14th February 2026	(2010 SE)	23rd September 2025
(2015 EG7)	26th April 2026	(2013 XS23)	18th December 2025
(2016 WJ1)	25th July 2026	484506 (2008 ER7)	26th February 2026
163132 (2002 CU11)	12th October 2026	(2017 KC36)	6th June 2026
(2013 XS23)	21st January 2027	(2013 QF11)	11th September 2026
168318 (1989 DA)	3rd May 2027	(2014 GE35)	26th November 2026
(2004 LB1)	18th August 2027	418849 (2008 WM64)	16th January 2027
(2009 DM45)	5th November 2027	(2012 EP10)	3rd April 2027
(2009 WC)	23rd January 2028	(2004 GD)	12th May 2027
(2014 BP43)	9th April 2028	(2013 NS13)	18th August 2027
(2015 FL)	20th June 2028	(2012 UB174)	29th November 2027
(2004 JV20)	6th August 2028	(2015 BH514)	14th March 2028
(2005 MA)	10th September 2028	(2009 UU1)	13th June 2028
(2012 EP10)	11th December 2028	(2015 XZ168)	12th August 2028
433953 (1997 XR2)	14th March 2029	(2012 RR16)	27th November 2029

2. the *Asteroid Lightcurve Database (LCDB)* presented by [11], containing sets of data generated from observational informations with the purpose to determine less known quantities to characterize the asteroids.

These two databases could be integrated [4] to obtain a set of suitable targets for future manned missions, and then used in the algorithm to design a precursor unmanned prospecting mission.

Compliance with Ethical Standards

Conflict of Interest On behalf of all authors, the corresponding author states that there is no conflict of interest.

References

1. Anthony, N., Reza Emami, M.: Asteroid engineering: the state-of-the-art of Near-Earth Asteroids science and technology. Prog. Aerosp. Sci. **100**, 1–17 (2018)
2. Di Carlo, M., Vasile, M.: Low-thrust tour of the main belt asteroids. Adv. Space Res. **62**, 2026–2045 (2017)
3. Izzo D., Hennes D., Simões L.F., Märtens M.: Designing complex interplanetary trajectories for the global trajectory optimization competitions. In: Fasano G., Pintér J. (eds) Space engineering. Springer optimization and its applications, vol. 114. Springer, Cham (2016). https://doi.org/10.1007/978-3-319-41508-6_6
4. Peloni, A., Dachwald, B., Ceriotti, M.: Multiple near-earth asteroid rendezvous mission: solar-sailing options. Adv. Space Res. **62**, 2084–2098 (2017). https://doi.org/10.1016/j.asr.2017.10.017
5. Fritz, S., Turkoglu, K.: Optimal trajectory determination and mission design for asteroid/deep space exploration via multi-body gravity assist maneuvers. In: 2016 IEEE aerospace conference, Big Sky, MT, 2016, pp. 1–9. https://doi.org/10.1109/AERO.2016.7500537
6. Park, R.S., Chamberlin, A.: Small-body database search engine, NASA Jet Propulsion Laboratory, https://ssd.jpl.nasa.gov/sbdb_query.cgi. Accessed Sept 2018
7. Williams, D.R.: Earth fact sheet, NASA Goddard Space Flight Center, https://nssdc.gsfc.nasa.gov/planetary/factsheet/earthfact.html. Accessed Sept 2018
8. Addis, B., Cassioli, A., Locatelli, M., Schoen, F.: Global optimization for the design of space trajectories. Comput. Optim. Appl. **48**, 635–652 (2011)
9. Di Carlo, M., Romero Martin, J.M., Vasile, M.: Automatic trajectory planning for low-thrust active removal mission in low-earth orbit. Adv. Space Res. **59**, 1234–1258 (2016)
10. Barbee, B.W., Esposito, T., Pinon, E., Hur-Diaz, S., Mink, R.G., Adamo, D.R.: A comprehensive ongoing survey of the Near-Earth Asteroid population for human mission accessibility, presentation at AIAA guidance, navigation and control conference of Toronto (2010)
11. Warner, B.D., Harris, A.W., Prave, P.: The asteroid lightcurve database. Icarus **202**, 134–146 (2009)